This article has been accepted for publication in a future proceedings of this conference, but has not been fully edited. Content may change prior to final publication. Citation information: DOI: 10.1109/ICASSPXXXXX.2023.000XXXXX, 2024 IEEE International Conference on Acoustics, Speech and Signal Processing (ICASSP 2024)

TOWARDS OPTIMIZED MULTI-CHANNEL MODULO-ADCS: MODULI SELECTION STRATEGIES AND BIT DEPTH ANALYSIS

Wenyi Yan† *Lu Gan*† *Shaoqing Hu*† *Hongqing Liu*‡

†Dept. of Electrical and Electronic Engineering, Brunel University, London, UK
‡School of Communication and Information Engineering,
Chongqing University of Posts and Telecommunications, Chongqing, China

ABSTRACT

This paper presents a theoretical analysis of multi-channel modulo analog-to-digital converters (ADCs) for high-dynamic range sampling under bounded noise. In particular, we derive the maximum error tolerance in terms of ADC dynamic range, signal dynamic range, and channel number. Additionally, we present closed-form expressions for ADC thresholds, ensuring near-optimal error resilience, and analyzing the minimal bit-depth needed for stable recovery. Compared to single-channel modulo ADCs, our approach achieves superior error tolerance with reduced sampling rates. Moreover, it demands a minor bit rate increase compared to conventional ADCs but operates with a significantly smaller ADC dynamic range.

***Index Terms*—** Analog-to-digital converters(ADC), modulo samplers, Chinese remainder theorem(CRT)

1. INTRODUCTION

Saturation or clipping issues pose challenges in various applications. For example, in high dynamic range photography, sunlit scenes often result in overexposure [1]. Similarly, in scientific imaging systems like ultrasound and radar, intense reflections risk overwhelming the sensors [2–6]. Additionally, in audio, clipping generates artifacts diminishing sound quality [7–9]. These complications stem from ADC's range limitations. Specifically, when input amplitudes surpass the ADC's threshold, described by $|f_{in}| > \frac{\Delta}{2}$ where Δ denotes the ADC's peak-to-peak range, the result is aliasing due to clipping. Consequently, output values are confined to $[-\frac{\Delta}{2}, +\frac{\Delta}{2}]$. To address this challenge, modulo ADCs have been developed [10, 11]. For an input $x \in \mathbb{R}$ and a threshold $\Delta > 0$, the modulo ADC wraps the input amplitude as:

$$\langle x \rangle_{\Delta} = x \mod \Delta = x - \Delta \left\lceil \frac{x}{\Delta} \right\rfloor \in \left[-\frac{\Delta}{2}, \frac{\Delta}{2} \right), \quad (1)$$

with $\lceil \cdot \rfloor$ denoting the rounding function. Single-channel modulo-ADC has been applied in areas like radar, imaging, and communications to increase dynamic range [12–14]. However, single-channel modulo-ADC system requires high sampling rates and computational costs.

Drawing on the Chinese Remainder Theorem (CRT), multi-channel modulo-ADC systems are introduced in [15, 16]. These systems promise reliable, high-dynamic range sampling even at low sampling rates. Illustrated in Fig. 1, an L-channel modulo-ADC system employs a sequence of distinct ADC thresholds $\Delta_1 < \Delta_2 < \cdots < \Delta_L = \Delta_{\max}$ defined as:

$$\Delta_l = \epsilon \tau_l, \quad 1 \le l \le L \quad (2)$$

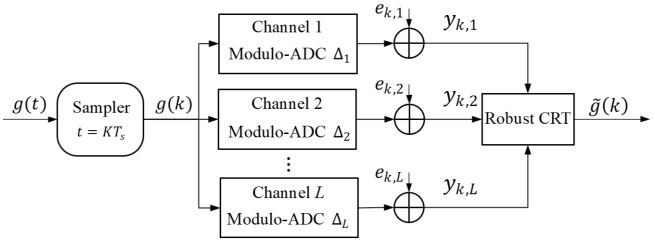

Fig. 1. Multi-channel modulo-ADC sampling architecture.

where ϵ is a positive floating-point number, and τ_l is pair-wise co-prime integer. Each channel samples at the Nyquist rate and the maximum signal amplitude P, is given by

$$P = \frac{\epsilon \tau_1 \tau_2 \cdots \tau_L}{2} \quad (3)$$

The robust CRT algorithms [17, 18] facilitate point-by-point, fast, and reliable signal reconstruction when the modulo ADC errors stay below $|e| < \epsilon/4$.

While multi-channel modulo-ADCs offer substantial promise, open questions remain about optimizing their performance. This paper analyzes and optimizes multi-channel modulo ADC systems to enable robust, high-dynamic range signal acquisition while keeping the bitrate overhead minimal. Our main contributions are:

- Deriving relationships between error tolerance, sampling rates, ADC dynamic range, and signal dynamic range to offer insights into multi-channel modulo system robustness and parameter selection;
- Providing closed-form expressions for the ADC thresholds for $L = 2, 3, 4$ that offer (near-) optimal resilience to errors, given the signal's peak magnitude $g_{\max}$ and the maximum ADC dynamic range $\Delta_{\max}$;
- The multi-channel modulo ADC architecture achieves high dynamic range signal acquisition with comparable hardware costs to conventional ADCs in terms of bits/sample.

The remainder of this paper is organized as follows. Section 2 reviews existing results on modulo ADC systems with bounded noises. Section 3 analyzes moduli selection and bitrates. Section 4 presents simulations of sampling bitrate, dynamic range, and channel number tradeoffs and concludes in Section 5.

Notations: Rational integers and natural numbers are represented by $\mathbb{Z}$ and $\mathbb{N}$, respectively. The ceiling and rounding operations for a real number x are given by $\lceil x \rceil$ and $\lfloor x \rfloor$. The greatest common divisor of two integers, p and q, is $\gcd(p, q)$. An integer p has a modular multiplicative inverse, q, if $pq \mod m = 1$.

Copyright © 2024 IEEE. Personal use of this material is permitted. Permission from IEEE must be obtained for all other uses, in any current or future media, including reprinting/republishing this material for advertising or promotional purposes, creating new collective works, for resale or redistribution to servers or lists, or reuse of any copyrighted component of this work in other works (see: https://journals.ieeeauthorcenter.ieee.org/become-an-ieee-journal-author/publishing-ethics/guidelines-and-policies/post-publication-policies/).

This article has been accepted for publication in a future proceedings of this conference, but has not been fully edited. Content may change prior to final publication. Citation information: DOI: 10.1109/ICASSPXXXXX.2023.000XXXXX, 2024 IEEE International Conference on Acoustics, Speech and Signal Processing (ICASSP 2024)

2. LITERATURE REVIEW

Consider an L-channel modulo ADC system characterized by ADC dynamic ranges $\Delta_1 < \Delta_2 < \ldots < \Delta_L = \Delta_{\max}$. Given a bandlimited input signal $g(t)$, the k-th sample (where $k \in \mathbb{Z}$) is defined as $g_k = g(k/f_s)$. Here, f_s represents the uniform sampling frequency across all channels. We set $g_{\max} = \|g(t)\|_\infty$ and express the noisy output for the k-th sample in the l-th channel as $y_{k,l} = \langle g_k \rangle_{\Delta_l} + e_{k,l}$, $1 \le l \le L$. Let $\|\boldsymbol{e}\|_\infty = \max_{k,l} |e_{k,l}|$ indicate the peak magnitude of ADC sample noise. In our context, the noise is bounded such that $\|\boldsymbol{e}\|_\infty < b_0$. If the reconstruction of the k-th sample is $\hat{g}_k$, then a **stable reconstruction** is defined by the relation:

$$\lceil \hat{g}_k/\Delta_l \rfloor = \lceil g_k/\Delta_l \rfloor \quad \forall\, k \in \mathbb{Z},\ 1 \le l \le L, \tag{4}$$

which further suggests that $|g_k - \hat{g}_k| \le \|\boldsymbol{e}\|_\infty$. In what follows, we summarize existing works of modulo-ADCs under bounded noises.

Single-channel modulo-ADCs ($L = 1$), commonly referred to as the unlimited sampling framework (USF), facilitate the perfect reconstruction of a bandlimited signal $g(t)$ from its oversampled modulo samples, as detailed in [11, 19]. Under noiseless conditions, a signal can be accurately recovered using the USF approach if the sampling rate meets the threshold of $f_T \ge 2\pi e f_{NYQ}$, where f_{NYQ} represents the Nyquist sampling rate [11]. Furthermore, Theorem 3 from [20] indicates that a bandlimited signal can be stably reconstructed from noisy modulo samples provided specific conditions are met. Specifically, with a sampling rate of $f_T > 2^\alpha \pi e f_{NYQ}$, stable recovery can be achieved given that the modulo ADC's noise is bounded by

$$\|\boldsymbol{e}\|_\infty \le \frac{\Delta_{\max}}{8}(2\rho)^{-\frac{1}{\alpha}}. \tag{5}$$

Here, α is a natural number, $\rho = 2g_{\max}/\Delta_{\max}$ is the amplitude scaling factor (also referred to as normalized dynamic range in [20]). The aforementioned bound demands a considerably high oversampling factor relative to the Nyquist rate. While empirical studies [11, 21–23] suggest that imposing extra constraints on $g(t)$ may allow for reduced sampling rates, to the best of our understanding, (5) represents the most robust theoretical bound for a generic bandlimited signal in a single-channel system.

Multi-channel modulo-ADC systems with $L > 1$ were first introduced in [15], leveraging a robust CRT recovery algorithm presented in [18, 24–27], as outlined in Algorithm 1. Within this framework, each channel samples at the Nyquist rate $f_s = f_{NYQ}$, resulting in a total sampling rate of $f_T = L f_{NYQ}$. Adopting Δ_l as specified in (2), stable reconstruction is attainable when $\|\boldsymbol{e}\|_\infty \le \frac{\epsilon}{4}$. A central challenge lies in optimizing τ_l to amplify ϵ given a specified $\Delta_{\max}$ and ρ. Additionally, there is a lack of study on the necessary bit rates. This paper aims to address these concerns.

It's worth noting that a dual-channel system ($L = 2$) was introduced in a recent study [28]. Unlike our CRT-based approach, their system requires that the ratio Δ_1/Δ_2 is an irrational number. However, implementing such a system in hardware poses challenges due to the inherent precision limitations of components. Moreover, the study did not address the noise robustness of their system [28].

3. MODULI SELECTION AND BITRATE ANALYSIS OF MULTI-CHANNEL ARCHITECTURE

3.1. Performance analysis for bounded noise

Theorem 1 presents the upper bound for noise tolerance in the context of a predetermined maximum threshold $\Delta_{\max}$ and amplitude scaling factor $\rho = 2g_{\max}/\Delta_{\max}$

Algorithm 1 Robust CRT reconstruction algorithm [18]

Input: ADC threshold parameters τ_l and ϵ, ADC modulo samples $y_{k,l} = \langle g_k \rangle_{\Delta_l} + e_{k,l}$

Output: Recovered estimate $\tilde{g}_k$

1: Compute $\gamma_1 = \prod_{l=2}^{L} \tau_j$

2: Compute $\hat{q}_{k,l,1} = \left\lceil \frac{y_{k,l} - y_{k,1}}{\epsilon} \right\rfloor,\ 2 \le l \le L$

3: Compute $\hat{\xi}_{k,l,1} = \hat{q}_{k,l,1}\bar{\tau}_{l,1} \pmod{\tau_l}$, where $\bar{\tau}_{l,1}$ is the multiplicative modulo inverse of $\tau_1 \pmod{\tau_l}$

4: Compute $\hat{n}_{k,1} = \sum_{l=2}^{L} \hat{\xi}_{k,l,1} b_{l,1} \frac{\gamma_1}{\tau_l} \pmod{\gamma_1}$, where $b_{l,1}$ is the modulo inverse of $\langle \frac{\gamma_1}{\tau_l} \rangle_{\tau_l}$

5: Compute $\hat{n}_{k,l} = \frac{\hat{n}_{k,1}\tau_1 - \hat{q}_{k,l,1}}{\tau_l}$

6: Compute $\tilde{g}_k = \frac{1}{L}\sum_{l=1}^{L} (\hat{n}_{k,l}\Delta_l + y_{k,l})$.

Theorem 1 (Multi-channel Modulo ADC Systems with Bounded Noise)**.** *Consider an L-channel modulo-ADC system (Fig. 1), with thresholds $\Delta_l = \tau_l \epsilon$, $1 \le l \le L$. Here, $\epsilon > 0$ and each τ_l are pairwise coprime integers. When each channel is sampled at its Nyquist rate, resulting in a total rate $f_T = L f_{NYQ}$, and let the k-th modulo sample in the l-th channel as $y_{k,l} = \langle g_k \rangle_{\Delta_l} + e_{k,l}$, with noise $e_{k,l}$. Stable reconstruction is achievable if the maximum error amplitude $\|\boldsymbol{e}\|_\infty = \max_{k,l} |e_{k,l}|$ satisfies:*

$$\|\boldsymbol{e}\|_\infty \le \frac{C\Delta_{max}}{4}\rho^{-\frac{1}{L-1}}, \tag{6}$$

where $\rho = 2g_{\max}/\Delta_{\max}$ is the amplitude scaling factor in (5) and $C < 1$ is a parameter determined by ρ and τ_l ($1 \le l \le L$). For large values of ρ, $C \approx 1$.

Proof. Due to space constraints, we outline the main steps. First, the maximum recoverable value P in (3) must exceed $g_{\max}$, i.e., $\frac{\tau_1\tau_2\ldots\tau_L\epsilon}{2} \ge g_{\max}$. Given the ADC's threshold restrictions, we also have: $\tau_L\epsilon \le \Delta_{\max}$. These lead to $\tau_1\tau_2\ldots\tau_{L-1} \ge \rho$ as well as $\epsilon \le \frac{\Delta_{\max}}{\tau_L}$. Recall from Algorithm 1, the modulo ADC's error needs to be bounded by $\|\boldsymbol{e}\|_\infty \le \frac{\epsilon}{4}$ for stable reconstruction. As ϵ is a positive real number, we can select $\epsilon = \frac{\Delta_{\max}}{\tau_L}$. For optimal error tolerance, τ_L is minimized under the constraints $\tau_1\tau_2\ldots\tau_{L-1} \ge \rho$, the order $\tau_1 \le \tau_2 \ldots \le \tau_{L-1} \le \tau_L$, and their pairwise co-primality. Therefore, each τ_l should be on the order of $\rho^{\frac{1}{L-1}}$. This makes $\epsilon = \frac{\Delta_{\max}}{\tau_L} = C\Delta_{\max}\rho^{-\frac{1}{L-1}}$ for some $C \approx 1$, validating (6). ■

Table 1 presents a comparative evaluation between the theoretical bounds of the single-channel system [11] and the proposed multi-channel modulo-ADC systems in terms of error tolerance and sampling rate. Notably, α in the single-channel system corresponds to $L - 1$ in its multi-channel counterpart. Both systems exhibit error tolerance orders of $\mathcal{O}\left(\rho^{-\frac{1}{L-1}}\right)$ and $\mathcal{O}\left(\rho^{-\frac{1}{\alpha}}\right)$, respectively. However, our multi-channel approach linearly increases the sampling rate with L, whereas the single-channel has an exponential dependence on α. This significant difference highlights that multi-channel modulo ADCs can achieve comparable error resilience to single-channel systems but with substantially lower sampling overhead. Therefore, the analysis substantiates the benefits of multi-channel architectures in attaining high dynamic range acquisition at low sampling frequencies.

Copyright © 2024 IEEE. Personal use of this material is permitted. Permission from IEEE must be obtained for all other uses, in any current or future media, including reprinting/republishing this material for advertising or promotional purposes, creating new collective works, for resale or redistribution to servers or lists, or reuse of any copyrighted component of this work in other works (see: https://journals.ieeeauthorcenter.ieee.org/become-an-ieee-journal-author/publishing-ethics/guidelines-and-policies/post-publication-policies/).

This article has been accepted for publication in a future proceedings of this conference, but has not been fully edited. Content may change prior to final publication. Citation information: DOI: 10.1109/ICASSPXXXXX.2023.000XXXXX, 2024 IEEE International Conference on Acoustics, Speech and Signal Processing (ICASSP 2024)

Table 1. Performance comparison of modulo-ADC systems under bounded noise, where f_T and $\|\boldsymbol{e}\|_\infty$ denote the total sampling rate and maximum error. Here, $\alpha \in \mathbb{N}$, $L \geq 2$ and $C < 1$.

System Type	f_T	$\|\boldsymbol{e}\|_\infty$
[11]	$\geq 2^\alpha \pi e f_{NYQ}$	$\leq \frac{\Delta_{\max}}{8}(2\rho)^{-\frac{1}{\alpha}}$
This work	Lf_{NYQ}	$\leq \frac{\Delta_{\max}}{4}\rho^{-\frac{1}{L-1}} \cdot C$

3.2. Moduli Selection

This subsection studies the (near-)optimal selection of τ_l and ϵ to enhance the system's error resilience. To address the interest in low oversampling factors, we provide closed-form solutions for $L = 2, 3$, and 4 in the following corollary.

Corollary 1. *Consider an L-channel modulo-ADC sampling system given in Theorem 1 with amplitude scaling factor of ρ and maximum ADC dynamic range of $\Delta_{\max}$. For $L = 2, 3$ and 4, τ_l $(1 \leq l \leq L)$ given below are pair-wise coprime and satisfy $\tau_l = \mathcal{O}(\rho^{\frac{1}{L}})$*

- *$L = 2$: $\tau_1 = \lceil \rho \rceil$, $\tau_2 = \tau_1 + 1$ and $\epsilon = \frac{\Delta_{max}}{\tau_2}$*
- *$L = 3$: $\tau_1 = 2a - 1$, $\tau_2 = 2a$, $\tau_3 = 2a + 1$ and $\epsilon = \frac{\Delta_{max}}{\tau_3}$, in which $a = \lceil (\sqrt{1 + 4\rho} + 1)/4 \rceil$ $(a > 1)$*
- *$L = 4$: $\epsilon = \frac{\Delta_{max}}{\tau_4}$ and there are two sets of solutions of τ_l $(1 \leq l \leq 4)$*
  - *$\tau_1 = 2a - 1$, $\tau_2 = 2a$, $\tau_3 = 2a + 1$, $\tau_4 = 2a + 3$ in which $a = \lceil 0.5\sqrt[3]{\rho} \rceil$, $a \mod 3 \neq 0$ and $a > 1$*
  - *$\tau_1 = 2a - 1$, $\tau_2 = 2a + 1$, $\tau_3 = 2a + 2$, $\tau_3 = 2a + 3$, in which $a = \lceil \sqrt[3]{5 + 0.125\rho} - 0.5 \rceil$, $a \mod 3 = 0$ and $a > 1$.*

Proof. For each value of L, we observe $\tau_L - \tau_1 \leq L$. This suggests that the τ_l values are closely grouped and have similar magnitudes. Given that $\prod_{l=1}^{L-1} \tau_l$ is roughly equivalent or slightly greater than ρ, it's clear that each τ_l is of the order $\mathcal{O}(\rho^{\frac{1}{L-1}})$.

To establish the pairwise coprime nature, it suffices to show that $\gcd(\tau_l, \tau_j) = 1$ for $1 \leq l < j \leq L$. Remember, for two integers p and q, their difference $p - q$ can be divided by $\gcd(p, q)$.

For $L = 2$, τ_1 and τ_2 are consecutive integers, ensuring they are coprime. For $L = 3$, one can show that $\gcd(\tau_1, \tau_2) = 1$ and $\gcd(\tau_2, \tau_3) = 1$ in a similar manner. Additionally, since both τ_1 and τ_3 are odd and their difference is 2, this confirms that they are relatively prime.

For $L = 4$, we build upon the conclusions derived from the $L = 3$ case. In the first set of solutions for τ_l where $1 \leq l \leq 4$: First, by applying the logic from the $L = 3$ discussion, we deduce that τ_1, τ_2, and τ_3 are pairwise co-prime. Then, for τ_3 and τ_4, their difference is 2. Since both are odd integers, they are not divisible by 2, implying $\gcd(\tau_3, \tau_4) = 1$. Next, the difference between τ_4 and τ_1 is 4. Both τ_1 and τ_4 being odd integers ensures they are not divisible by 2 or 4. This establishes that $\gcd(\tau_1, \tau_4) = 1$. Finally, analyzing τ_4 and τ_2, we see that their difference, $\tau_4 - \tau_2 = 3$. Given the condition $a \mod 3 \neq 0$, neither $\tau_2 = 2a$ nor $\tau_4 = 2a + 3$ are divisible by 3. This confirms $\gcd(\tau_2, \tau_4) = 1$.

For the second set of solutions for $L = 4$, the pairwise coprime property can be proved using a similar approach. ■

In Table 2, we compare the single-channel modulo ADC system from [11] against our multi-channel system for $\Delta_{\max} = 40$ and varying ρ. At $\rho = 10$, the single-channel requires up to $34.3 f_{NYQ}$ for an error tolerance of 1.11, whereas our system, with three channels, uses only $3f_{NYQ}$ to achieve an error of 2. For $\rho = 100$, our two-channel setup attains a 0.099 error at just $2f_{NYQ}$, contrasting with the single-channel's 0.025 error at $17.1 f_{NYQ}$. Overall, our CRT-based multi-channel system consistently achieves a larger error tolerance with significantly reduced sampling rates compared to the single-channel modulo ADC.

Table 2. Comparison of modulo-ADC systems under bounded noise, where $\Delta_{\max} = 40$, f_T and $\|\boldsymbol{e}\|_\infty$ denote the sampling rate ADC error tolerance, respectively

ρ	Systems	L	τ_l	α	$\|\boldsymbol{e}\|_\infty$	f_T
10	[11]	1	-	1	0.25	$17.1 f_{NYQ}$
		1	-	2	1.11	$34.3 f_{NYQ}$
	Ours	2	10, 11	-	0.91	$2f_{NYQ}$
		3	3, 4, 5	-	2	$3f_{NYQ}$
100	[11]	1	-	1	0.025	$17.1 f_{NYQ}$
		1	-	2	0.35	$34.3 f_{NYQ}$
	Ours	2	100, 101	-	0.099	$2f_{NYQ}$
		3	11,12,13	-	0.77	$3f_{NYQ}$

3.3. Bit depth analysis

In this subsection, we analyze the bit rate for the multi-channel system, focusing on the minimum bits needed for stable recovery.

Corollary 2. *For an L-channel modulo-ADC system as specified in Theorem 1, with amplitude scaling factor ρ and ADC dynamic ranges $\Delta_l = \tau_l \epsilon$ $(1 \leq l \leq L)$. Assuming that a mid-rise uniform quantizer is used with b bits per modulo-ADC sample (totaling $B = Lb$ bits per signal sample), stable reconstruction requires*

$$b \geq \log_2 \tau_L + 1. \tag{7}$$

If B_c represents bits per signal sample in a conventional ADC without saturation (with the same quantization step) and let $\eta = B/B_c$ denote the bit-rate oversampling factor, then

$$B_c = b + \log_2 \rho \quad \textit{and} \quad \eta = \frac{Lb}{b + \log_2 \rho} \tag{8}$$

Proof. Given the maximum dynamic range of the ADC system as $\Delta_{\max}$, the quantization step is defined by $q = \frac{\Delta_{\max}}{2^b}$. With the maximum quantization error capped at $\frac{q}{2}$, a stable reconstruction requires that $\epsilon/4 \geq \Delta_{\max}/2^{b+1}$. Substituting $\epsilon = \Delta_{\max}/\tau_L$ yields (7). For a conventional ADC with the same quantization step, the relation $2g_{\max}/2^{B_c} = \Delta_{\max}/2^b$ leads to (8). ■

The Corollary specifies the minimum bit requirement for stable signal reconstruction and compares it to a conventional ADC without clipping. Specifically:

Bit-depth requirement Eq. (7) suggests the minimum bit requirement is $b_{\min} = \log_2 \tau_L + 1$. Let $\tau_L = c_L \rho^{\frac{1}{L-1}}$ $(c_L > 1)$, one can derive that for every signal sample, the minimum number of required bits $B_{min} = Lb_{min}$ is

$$B_{\min} = \frac{L}{L-1} \log_2 \rho + L(1 + \log_2 c_L), \tag{9}$$

Building on the parameters given in Corollary 1, we plot the relationship between ρ and $B_{\min}$ for $L = 2, 3$ and 4 in Fig. 2. One can observe that for when $\rho < 60$, a 2-channel system requires the least

Copyright © 2024 IEEE. Personal use of this material is permitted. Permission from IEEE must be obtained for all other uses, in any current or future media, including reprinting/republishing this material for advertising or promotional purposes, creating new collective works, for resale or redistribution to servers or lists, or reuse of any copyrighted component of this work in other works (see: https://journals.ieeeauthorcenter.ieee.org/become-an-ieee-journal-author/publishing-ethics/guidelines-and-policies/post-publication-policies/).

This article has been accepted for publication in a future proceedings of this conference, but has not been fully edited. Content may change prior to final publication. Citation information: DOI: 10.1109/ICASSPXXXXX.2023.000XXXXX, 2024 IEEE International Conference on Acoustics, Speech and Signal Processing (ICASSP 2024)

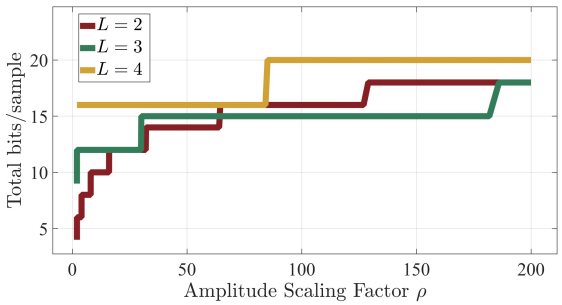

Fig. 2. The evolution of minimum precision B in different multi-channel system recovery as ρ varied from 2 to 200.

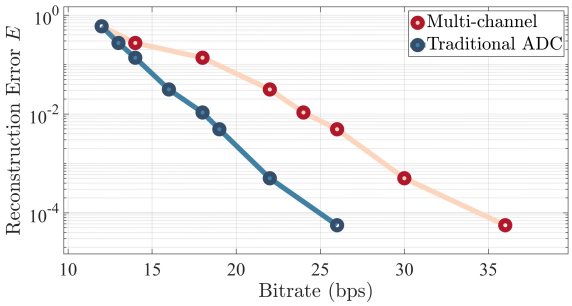

Fig. 3. Comparison of total bitrate vs. distortion: our 2-channel modulo-ADCs ($\Delta_{\max} = 150$) vs. conventional ADC ($\Delta_{\max} = 4000$) at peak amplitude $g_{\max} = 2000$.

total bits. But as ρ increases, a 3-channel configuration emerges as the optimal choice. This observation furnishes crucial insights for the selection of modulo-ADC parameters in practical applications.

Comparison with Conventional ADCs: In an L-channel modulo ADC system, despite the frequency oversampling factor being L, the bit rate factor η is always less than L, i.e., $\eta < L$, as shown in Eq. (8). For a given b and L, a larger ρ reduces η, highlighting efficiency at high ρ. Given L and ρ, η grows with the increase of b. Thus, high-resolution quantizers lead to higher η, while low-resolution ones reduce overhead. The lowest η occurs at $b = b_{\min}$, and the conventional ADC's bit requirement is:

$$B_{c,\min} = B_{\min} - (L-1)(1 + \log_2 c_L) \tag{10}$$

Considering $c_L > 1$, $B_{c,\min}$ is less than $B_{\min}$, implying $\eta > 1$ and denoting a higher bit demand in modulo-ADCs compared to conventional ones. For an optimal system with $c_L \approx 1$, $B_{\min}$ is close to $B_{c,\min} + L$, indicating a minor addition of L bits per sample. Especially for small L values (2 to 4), this slight increase in bit rate is offset by a notable rise in dynamic range, suggesting significant potential in practical applications.

4. SIMULATION RESULTS

In this section, we compare the performance of different ADC systems under quantization noises, including: *i*) Our 2-channel modulo ADC system; *ii*) Single-channel modulo ADC system; and *iii*) conventional ADC system without saturation. The input band-limited signal takes the following form:

$$g(t) = \sum_{i=-30}^{30} A \cdot a_i \cdot \mathrm{sinc}(t - i), \tag{11}$$

The coefficients a_i follow a uniform distribution within the interval [-1,1], and A is a normalization factor such that $g_{\max} = 2000$. For modulo ADC systems, we set $\Delta_{\max} = 150$, resulting in an amplitude scaling factor of $\rho = 2g_{\max}/\Delta_{\max} \approx 26.7$. Utilizing Corollary 1, we choose $\tau_1 = 27$, $\tau_2 = 28$, and $\epsilon = 150/28 \approx 5.36$ in our system. Each channel is sampled at the Nyquist rate $f_s = 1$ Hz, resulting in a total sampling rate of $f_T = 2$ Hz. For the single-channel modulo ADC system and conventional ADC system, the sampling frequencies are $f_T = 18.2$ Hz and $f_T = 1$ Hz, respectively. We quantify the performance based on the maximum distortion of the reconstructed signal.

$$E = \max_k |\tilde{g}(k) - g(k)| \tag{12}$$

Table 3. Bitrate Analysis

System Type	$\Delta_{\max}$	L	E	Bitrate	f_T
[11]	150	1	10^{-3} 10^{-1}	309 bps 163 bps	18.2 Hz
Conventional ADCs	4,000	1	10^{-3} 10^{-1}	22 bps 14 bps	1 Hz
Ours	150	2	10^{-3} 10^{-1}	30 bps 18 bps	2 Hz

In Fig.3, we compare the total bit rates of our 2-channel modulo ADC system with those of a conventional ADC. Despite doubling the sampling rate, our modulo ADC system requires only a slight increase in bit rate. This is particularly noteworthy because our system operates with a significantly reduced ADC dynamic range compared to conventional ADCs. Table3 provides a more detailed comparison of bit-rate requirements among various ADC frameworks. For the same distortion levels, our system's bit rate is slightly higher than that of traditional ADCs but significantly lower than that of the single-channel modulo ADC, highlighting its practical potential.

5. CONCLUSIONS AND FUTURE WORK

In this paper, we provide a comprehensive theoretical analysis of multi-channel modulo-ADC systems under bounded noise, leveraging a robust CRT reconstruction algorithm [18]. We derive the maximum error tolerance of the ADC in terms of its dynamic range, maximum signal amplitude, and number of channels. Additionally, we present the closed-form expressions of ADC thresholds required to achieve (near-) optimal error resilience, followed by an analysis of bit depth. In comparison to single-channel ADC systems [20], our system offers a larger error tolerance at a much lower sampling frequency. While it requires a marginal increase in bit rate compared to conventional ADC systems, it operates with a significantly reduced ADC dynamic range at comparable distortion levels.

In the future, we aim to conduct error analysis using advanced reconstruction techniques like lattice-based methods [15]. We also plan to explore practical hardware integrations and radar applications.

Copyright © 2024 IEEE. Personal use of this material is permitted. Permission from IEEE must be obtained for all other uses, in any current or future media, including reprinting/republishing this material for advertising or promotional purposes, creating new collective works, for resale or redistribution to servers or lists, or reuse of any copyrighted component of this work in other works (see: https://journals.ieeeauthorcenter.ieee.org/become-an-ieee-journal-author/publishing-ethics/guidelines-and-policies/post-publication-policies/).

This article has been accepted for publication in a future proceedings of this conference, but has not been fully edited. Content may change prior to final publication. Citation information: DOI: 10.1109/ICASSPXXXXX.2023.000XXXXX, 2024 IEEE International Conference on Acoustics, Speech and Signal Processing (ICASSP 2024)

6. REFERENCES

[1] Yujie Mei and Guoping Qiu, "Recovering High Dynamic Range Radiance Maps from Photographs Revisited: A Simple and Important Fix," in *2013 Seventh International Conference on Image and Graphics*, 2013, pp. 23–28.

[2] Huanxue Zhou Donghui Hu and Wen Hong, "Correction method for saturated SAR data to improve radiometric accuracy," in *Proceedings. 2005 IEEE International Geoscience and Remote Sensing Symposium, 2005. IGARSS '05.*, July 2005, vol. 5, pp. 3344–3347, ISSN: 2153-7003.

[3] Yichen Li, Majid Safari, Robert Henderson, and Harald Haas, "Optical OFDM with single-photon avalanche diode," *IEEE Photonics Technology Letters*, vol. 27, pp. 943–946, 5 2015.

[4] Ziang Liu, Sundar Aditya, Hongyu Li, and Bruno Clerckx, "Joint transmit and receive beamforming design in full-duplex integrated sensing and communications," *IEEE Journal on Selected Areas in Communications*, vol. 41, no. 9, pp. 2907–2919, 2023.

[5] K. Yamada, T. Nakano, and S. Yamamoto, "A vision sensor having an expanded dynamic range for autonomous vehicles," *IEEE Transactions on Vehicular Technology*, vol. 47, no. 1, pp. 332–341, 1998.

[6] Haley M. So, Julien N.P. Martel, Gordon Wetzstein, and Piotr Dudek, "Mantissacam: Learning snapshot high-dynamic-range imaging with perceptually-based in-pixel irradiance encoding," in *2022 IEEE International Conference on Computational Photography (ICCP)*, 2022, pp. 1–12.

[7] Amir Adler, Valentin Emiya, Maria G. Jafari, Michael Elad, Rémi Gribonval, and Mark D. Plumbley, "Audio inpainting," *IEEE Transactions on Audio, Speech and Language Processing*, vol. 20, pp. 922–932, 2012.

[8] Abdelhakim Dahimene, M. Noureddine, and Arab Azrar, "A simple algorithm for the restoration of clipped speech signal," *Informatica (Slovenia)*, vol. 32, pp. 183–188, 2008.

[9] Simon J. Godsill, Patrick J. Wolfe, and William N.W. Fong, "Statistical model-based approaches to audio restoration and analysis," *International Journal of Phytoremediation*, vol. 21, pp. 323–338, 2001.

[10] Dongwon Park, Jehyuk Rhee, and Youngjoong Joo, "A wide dynamic-range CMOS image sensor using self-reset technique," *IEEE Electron Device Letters*, vol. 28, pp. 890–892, 10 2007.

[11] Ayush Bhandari, Felix Krahmer, and Ramesh Raskar, "Unlimited sampling of sparse signals," in *2018 IEEE International Conference on Acoustics, Speech and Signal Processing (ICASSP)*, 2018, pp. 4569–4573.

[12] Thomas Feuillen, Mohammad Alaee-Kerahroodi, Ayush Bhandari, M. R. Bhavani Shankar, and Björn Ottersten, "Unlimited sampling for FMCW radars: A proof of concept," 2022, Institute of Electrical and Electronics Engineers.

[13] Feng Ji, Pratibha, and Wee Peng Tay, "Unlimited dynamic range signal recovery for folded graph signals," *Signal Processing*, vol. 198, pp. 108574, 2022.

[14] Ziang Liu, Ayush Bhandari, and Bruno Clerckx, "λ–mimo: Massive MIMO via modulo sampling," *IEEE Transactions on Communications*, pp. 1–1, 2023.

[15] Lu Gan and Hongqing Liu, "High Dynamic range sensing using multi-channel modulo samplers," in *2020 IEEE 11th Sensor Array and Multichannel Signal Processing Workshop (SAM)*, 2020, pp. 1–5.

[16] Yicheng Gong, Lu Gan, and Hongqing Liu, "Multi-channel Modulo Samplers Constructed from Gaussian Integers," *IEEE Signal Processing Letters*, vol. 28, pp. 1828–1832, 2021.

[17] Hanshen Xiao, Yufeng Huang, Yu Ye, and Guoqiang Xiao, "Robustness in chinese remainder theorem for multiple numbers and remainder coding," *IEEE Transactions on Signal Processing*, vol. 66, no. 16, pp. 4347–4361, 2018.

[18] Wenjie Wang and Xiang-Gen Xia, "A closed-form robust chinese remainder theorem and its performance analysis," *IEEE Transactions on Signal Processing*, vol. 58, no. 11, pp. 5655–5666, 2010.

[19] Ayush Bhandari and Felix Krahmer, "On identifiability in unlimited sampling," in *2019 13th International conference on Sampling Theory and Applications (SampTA)*, 2019, pp. 1–4.

[20] Ayush Bhandari, Felix Krahmer, and Ramesh Raskar, "On unlimited sampling and reconstruction," *IEEE Transactions on Signal Processing*, vol. 69, pp. 3827–3839, 2021.

[21] Ayush Bhandari, Felix Krahmer, and Thomas Poskitt, "Unlimited sampling from theory to practice: Fourier-prony recovery and prototype ADC," *IEEE Transactions on Signal Processing*, vol. 70, pp. 1131–1141, 2022.

[22] Thomas Feuillen, Bhavani Shankar MRR, and Ayush Bhandari, "Unlimited sampling radar: Life below the quantization noise," in *ICASSP 2023 - 2023 IEEE International Conference on Acoustics, Speech and Signal Processing (ICASSP)*, 2023, pp. 1–5.

[23] Ayush Bhandari and Felix Krahmer, "HDR imaging from quantization noise," in *2020 IEEE International Conference on Image Processing (ICIP)*, 2020, pp. 101–105.

[24] Li Xiao, Xiang Gen Xia, and Wenjie Wang, "Multi-stage robust chinese remainder theorem," *IEEE Transactions on Signal Processing*, vol. 62, pp. 4772–4785, 9 2014.

[25] Xiaoping Li, Xiang-Gen Xia, Wenjie Wang, and Wei Wang, "A robust generalized Chinese Remainder Theorem for two integers," *IEEE Transactions on Information Theory*, vol. 62, no. 12, pp. 7491–7504, 2016.

[26] Li Xiao, Xiang-Gen Xia, and Haiye Huo, "Towards robustness in residue number systems," *IEEE Transactions on Signal Processing*, vol. 65, no. 6, pp. 1497–1510, 2017.

[27] Wenjie Wang, Xiaoping Li, Wei Wang, and Xiang-Gen Xia, "Maximum likelihood estimation based robust Chinese Remainder Theorem for real numbers and its fast algorithm," *IEEE Transactions on Signal Processing*, vol. 63, no. 13, pp. 3317–3331, 2015.

[28] Ruiming Guo and Ayush Bhandari, "Unlimited Sampling of FRI Signals Independent of Sampling Rate," in *ICASSP 2023 - 2023 IEEE International Conference on Acoustics, Speech and Signal Processing (ICASSP)*, 2023, pp. 1–5.

Copyright © 2024 IEEE. Personal use of this material is permitted. Permission from IEEE must be obtained for all other uses, in any current or future media, including reprinting/republishing this material for advertising or promotional purposes, creating new collective works, for resale or redistribution to servers or lists, or reuse of any copyrighted component of this work in other works (see: https://journals.ieeeauthorcenter.ieee.org/become-an-ieee-journal-author/publishing-ethics/guidelines-and-policies/post-publication-policies/).